GEOGRAPHICAL REPORTS
OF TOKYO METROPOLITAN UNIVERSITY 58 (2023) 95–102

SURFACE AIR TEMPERATURE RESPONSE TO INCREASING ANTHROPOGENIC AEROSOLS IN ASIAN MONSOON REGION IN BOREAL WINTER

Sho KITABAYASHI and Hiroshi G. TAKAHASHI

Abstract This study investigated the surface air temperature (SAT) response to increasing anthropogenic aerosol (AA) by separating it into fast and slow responses using the Coupled Model Intercomparison Project Phase 6 climate model outputs. Although an increase in AA generally contributes to cooling SAT over and around the source regions, this study focused on some notable responses, particularly unexpected warming signals over South Asia. In boreal winter, the slow response of SAT contributed to the relative warming over and around India, whereas the fast response did not. As the slow response, a decrease in cloud fraction, enhancement of downward anomalous motion, and an increase in downward radiation flux anomaly at the surface were found, which corresponded to the relative warming, although none of these occurred as fast response. These results suggest that processes mediated by sea surface temperature and clouds are critical for the relative warming over South Asia in boreal winter.

Keywords: anthropogenic aerosol, surface air temperature, Asian monsoon, boreal winter, fast/slow responses

1. Introduction

Aerosols have a significant influence on global and regional climates. Aerosols scatter and reflect or absorb incoming solar radiation, which alters the radiation budget through aerosol–radiation interaction (ARI) and aerosol–cloud interaction (ACI). Examining the radiative effects of aerosols is important to understand their current climate impact as well as future climate projections. The understanding of the climate impact of aerosol radiative forcing has recently improved; however, it still remains uncertainty (Forster *et al.* 2021).

The Asian monsoon (AM) region is one of the largest sources of anthropogenic aerosols (AAs) (Li *et al.* 2016). AA forcing altered the Asian summer monsoon (ASM) precipitation and circulation (e.g., Bollasina *et al.* 2011; Ganguly *et al.* 2012). Several studies have proposed that separation of fast and slow responses apply to evaluate the response to AA (e.g., Andrews *et al.* 2010). A fast response is a direct atmospheric effect in response to AA. Whereas, slow response is response to aerosol-induced radiative forcing with sea surface temperature (SST) change. Previous studies have shown that slow response to increasing AAs is an important factor in the weakening of ASM. Wang *et al.* (2019) evaluated the responses of ASM precipitation and circulation to increasing AAs by separating fast and slow responses using multiple climate model simulations. Their results showed that the South Asian summer monsoon (SASM) precipitation was weakened, and that the contribution of slow response was more dominant than that of fast response. They also investigated

various SST patterns and found that the interhemispherical meridional SST gradient pattern was significant for the slow response that weakened SASM precipitation, and that the tropical Indian Ocean SST change pattern also contributed partly.

Although AM precipitation and circulation responses to increasing AAs have been investigated, more investigations are warranted due to their complexity, particularly in boreal winter. Also, although the response of surface air temperature (SAT) to increasing AAs in the AM region would be simpler, it has yet to be well understood because the SAT response can interact with the AM cloud, precipitation and circulation. Therefore, we investigated the SAT response to increasing AAs in boreal winter by separating fast and slow responses using climate model simulation datasets from the Coupled Model Intercomparison Project Phase 6 (CMIP6; Eyring *et al.* 2016). The rest of the paper is organized as follows: section 2 introduces the datasets and methodology, section 3 evaluates the responses of SAT and other variables to increasing AAs in boreal winters, and section 4 summarizes the study.

2. Data and Methods

To reduce uncertainties induced by internal variability and model biases, we used multimodel ensembles of the CMIP6 simulation outputs (listed in Table 1). They performed all of the following experiments: basic Coupled General Circulation Model (CGCM) historical simulation from 1850 (HIST); HIST with AA-forcing fixed at the preindustrial era level (piAer); and two Atmospheric GCM (AGCM) experiments, corresponding to HIST (histSST) and piAer (SSTpiAer). The experiments were conducted within the framework of the Aerosol Chemistry Model Intercomparison Project (AerChemMIP; Collins *et al.* 2017). The total, fast, and slow responses were calculated using these four experiments. The total response (X_{total}; where X denotes the variable name, such as SAT, and subscript denotes the name of experiment/response) can be obtained by the difference between HIST and piAer ($X_{\mathrm{total}} = X_{\mathrm{HIST}} - X_{\mathrm{piAer}}$). Similarly, the fast response (X_{fast}) can be obtained by the difference between histSST and SSTpiAer ($X_{\mathrm{fast}} = X_{\mathrm{histSST}} - X_{\mathrm{SSTpiAer}}$) and the slow response (X_{slow}) can be obtained by the difference between the total and fast responses ($X_{\mathrm{slow}} = X_{\mathrm{total}} - X_{\mathrm{fast}}$).

Table 1 CMIP6 Climate Models Used for the Analysis

Model Name	Institute
GFDL-ESM4.0	Geophysical Fluid Dynamics Laboratory
GISS-E2.1-G	Goddard Institute for Space Studies
MIROC6	MIROC Consortium: JAMSTEC, AORI, NIES, R-CCS
MPI-ESM1.2-HAM	Max Planck Institute for Meteorology
MRI-ESM2.0	Meteorological Research Institute Japan
NorESM2-LM	NorESM Climate Modelling Consortium
UKESM1.0-LL	Met Office Hadley Centre

The analysis period was 1981–2010, and the analyzed variables were SAT, SST, downward shortwave radiation flux at the surface (DSRS), cloud fraction (CL), and vertical pressure velocity

(ω). The climatological mean for 1981–2010 was calculated for each experiment, and the total, fast, and slow responses were calculated for each variable. Each modelensemble was regridded to 2.5° × 2.5° at a horizontal resolution.

Statistical significance was evaluated using the sign test. For the multimodel mean response, we quantified the level of model agreement based on the sign of the response. If all seven modelensembles agree on the sign of the signals, then they are considered to exceed the 98% confidence level.

3. Results

Total, Fast, and Slow Responses of SAT to Increasing AAs

This section confirmed the total, fast, and slow responses of SAT to increasing AAs during December–February (DJF). First, we confirmed the spatial distribution of the increasing AAs. Figure 1 shows the amount of AAs increased from the preindustrial era. The aerosol optical depth at 550 nm (AOD) has increased globally since the preindustrial era. The increasing AAs were also clearly observed in Europe, Asia and North America, and their distribution leaned toward the Northern Hemisphere. Due to recent economic development in Asia, notable increase in AAs were found, particularly over East and South Asia. The increase in AAs was particularly significant (> 1) in East Asia.

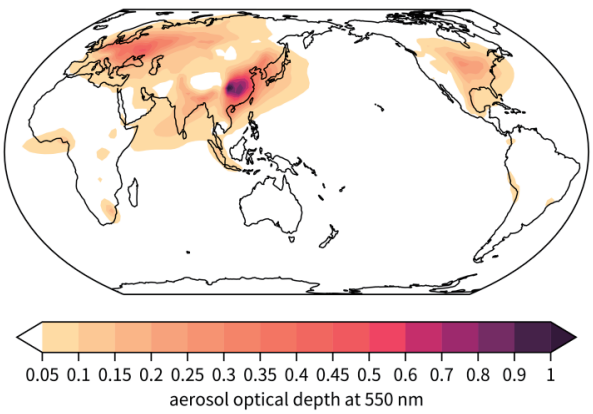

Fig. 1 Spatial distribution of multimodel mean AOD representing increased AAs in DJF. The anomalies were obtained as the differences between AOD_{hist} and AOD_{piAer}.

Figures 2a–c show the global SAT_{total}, SAT_{fast}, and SAT_{slow} in DJF, respectively. From a global perspective, the distribution of SAT_{total} is similar to that of SAT_{slow}. The decrease in SAT_{slow} was significant in the Northern Hemisphere, unlike in the Southern Hemisphere. SAT_{slow} consisted of an interhemispherical gradient pattern owing to the non-uniform distribution of the AA source. This finding is consistent with the results of previous studies. Focusing on the regional scale, SAT decreases were found in the regions with higher AOD (Fig. 1) although SAT_{fast} was weaker than SAT_{slow}. Thus, to explain the total SAT responses, we should consider both fast and slow responses.

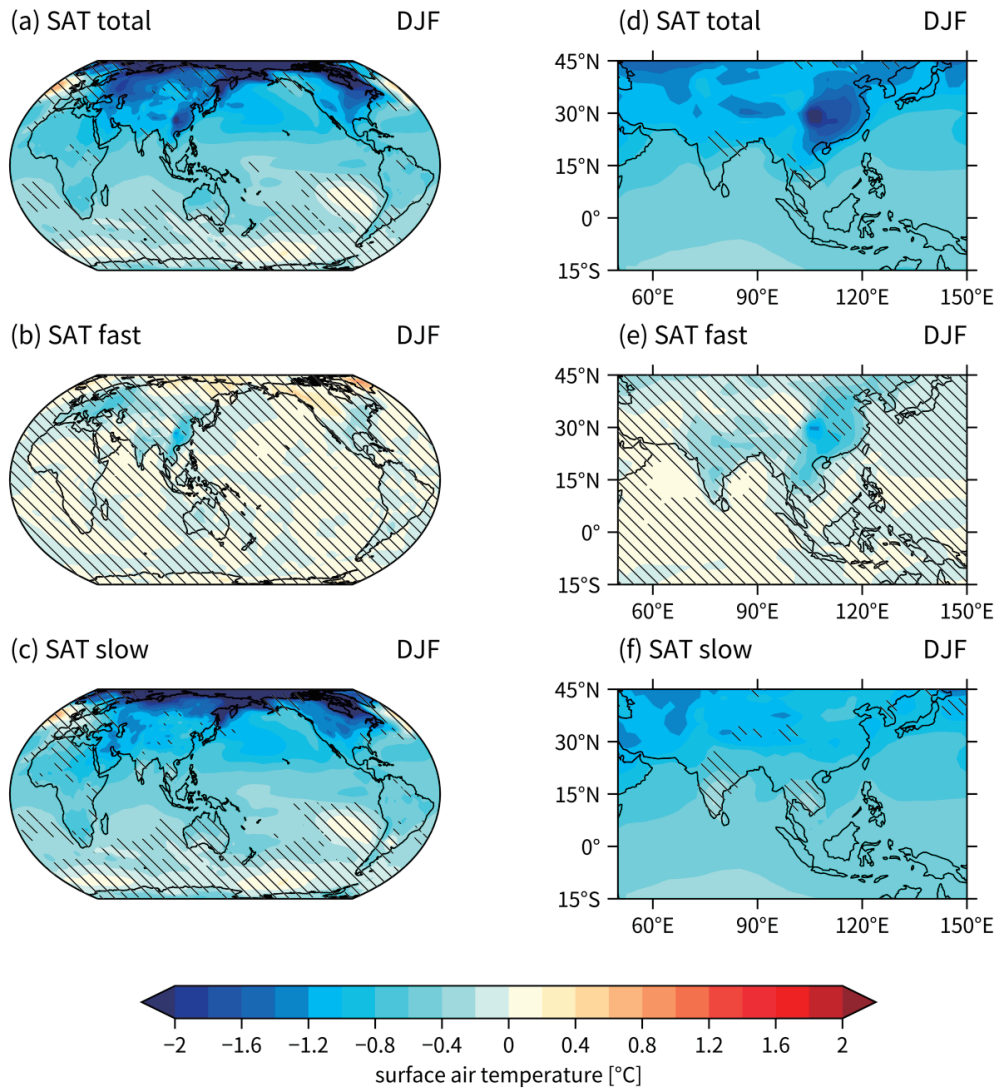

Fig. 2 **(a, d)** Total, **(b, e)** fast, and **(c, f)** slow responses of SAT, plotted **(a–c)** global distribution and **(d–f)** AM region distribution. Hatching indicates regions with below 98% significance by sign test (not all modelensembles agreed on the sign).

Figures 2d–f show the SAT responses in AM region. The SAT_{total} and SAT_{slow} decreased in almost all AM regions. However, the decrease in SAT over and around India was weaker, as compared to other AM regions.

For the fast response, the decrease in SAT was located over South and East Asia, which is the source of AA. In particular, the SAT decrease over East Asia was significant and contributed to a considerable decrease in SAT_{total}. The relative SAT warming over and around India induced by the fast response was small.

Responses of Cloud and Vertical Wind

In the previous section, we confirmed the total, fast, and slow SAT responses. Here, we investigated the responses of other variables (CL and vertical winds) considered to be relevant to relative warming over South Asia (Fig. 3).

Focusing over and around India, the decrease in CL was found by total and slow responses (Figs. 3a, c). The latitudinal region of decrease in CL corresponded to the latitude that induced anomalous downward motions (Figs. 3d, f). As the slow response, the anomalous 850-hPa winds were northeasterlies or easterlies, which indicates a slight enhancement of the climatological winter monsoon circulations. Anomalous downward motion was found from the bottom to the top of the troposphere, which enhanced the tropospheric meridional circulation of the rising over the South Indian Ocean and sinking in the south of the Indian subcontinent. Thus, the decrease in CL in this region was coupled with the modulation of vertical motions induced by the slow responses. However, the decrease in CL_{fast} over and around India was not found, and the anomalous upward motion appeared (Figs. 3b, e). For north of 30°N, the signals of ω_{fast} were opposite to ω_{slow}.

DSRS Responses

Generally, SAT change was significantly influenced by changes in radiation fluxes. Figure 4 shows the spatial distributions of all-sky DSRS (DSRSall), clear-sky DSRS (DSRScs), and the difference of DSRSall and DSRScs (DSRScld) for each response. Because DSRScs is recalculated DSRS without clouds, DSRScld represents the DSRS related to cloud radiative forcing. Thus, DSRScs can mostly be considered as ARI and DSRScld to ACI (Fig. 4f).

$DSRSall_{total}$ and $DSRSall_{fast}$ were decreased all over the AM region (Figs. 4a, b). Over and around India, $DSRS_{total}$ and $DSRS_{fast}$ were primarily contributed by non-cloud-related processes (Figs. 4d, e). $DSRScs_{fast}$ had a similar distribution to that of AOD (Fig. 1), which was significantly affected by the ARI. On the other hand, $DSRScld_{fast}$ over and around India was very small, which indicates that the cloud forcing is weak in the fast response. It was notable that DSRScld increased over the source of AA in East Asia, in particular the fast response was dominant. Thus, over the source of AA, clouds decreased despite the large supply of AA.

$DSRScs_{slow}$ was very weak because atmospheric direct effects such as ARI were mostly explained by the $DSRS_{fast}$. Thus, the $DSRS_{slow}$ was influenced by the cloud-related response to AA. Nevertheless, $DSRScs_{slow}$ slightly increased around India, Bay of Bengal, and Southeast Asia. Thus, both non-cloud-related and cloud-related processes contributed to the increase in $DSRS_{slow}$ over and around India.

Considering the results in the previous section, the $DSRS_{slow}$ was likely to be influenced by the decrease in CL and anomalous downward motions, induced by the slow response. Thus, the slow responses of clouds, atmospheric circulation, and incoming solar radiation at the surface may be critical to relative warming over and around India.

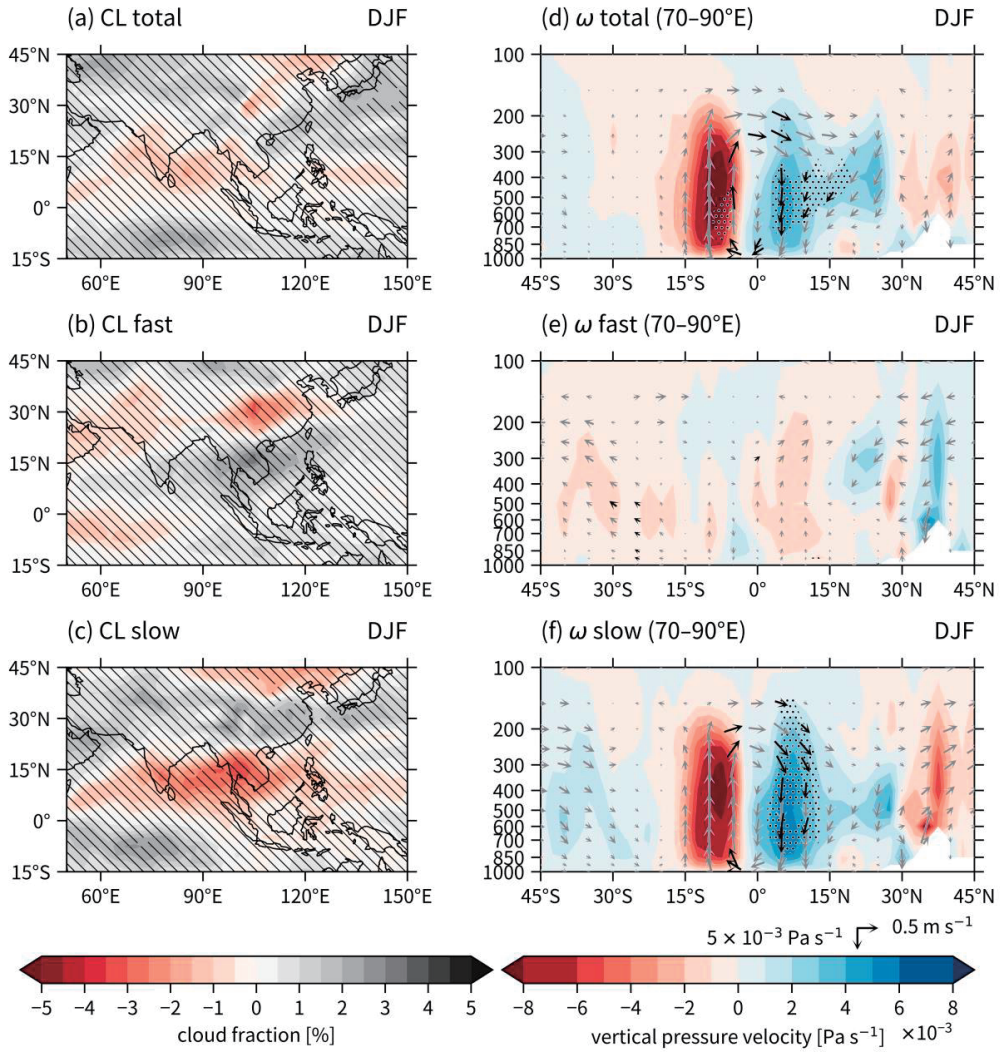

Fig. 3 **(a, d)** Total, **(b, e)** fast, and **(c, f)** slow responses of **(a–c)** CL, **(d–f)** ω (shade), and meridional–vertical wind (vector). Zonal–meridional wind and ω were zonal mean for the region including the Indian subcontinent (70–90°E). **(a–c)** Hatching indicates regions with below 98% significance by sign test (not all modelensembles agreed on the sign). **(d–f)** Black and gray vectors represent regions which exceed 98% significant (all modelensembles agreed on the sign) or not, respectively; Dotted region in indicates regions where the response of ω is below 98% significance level.

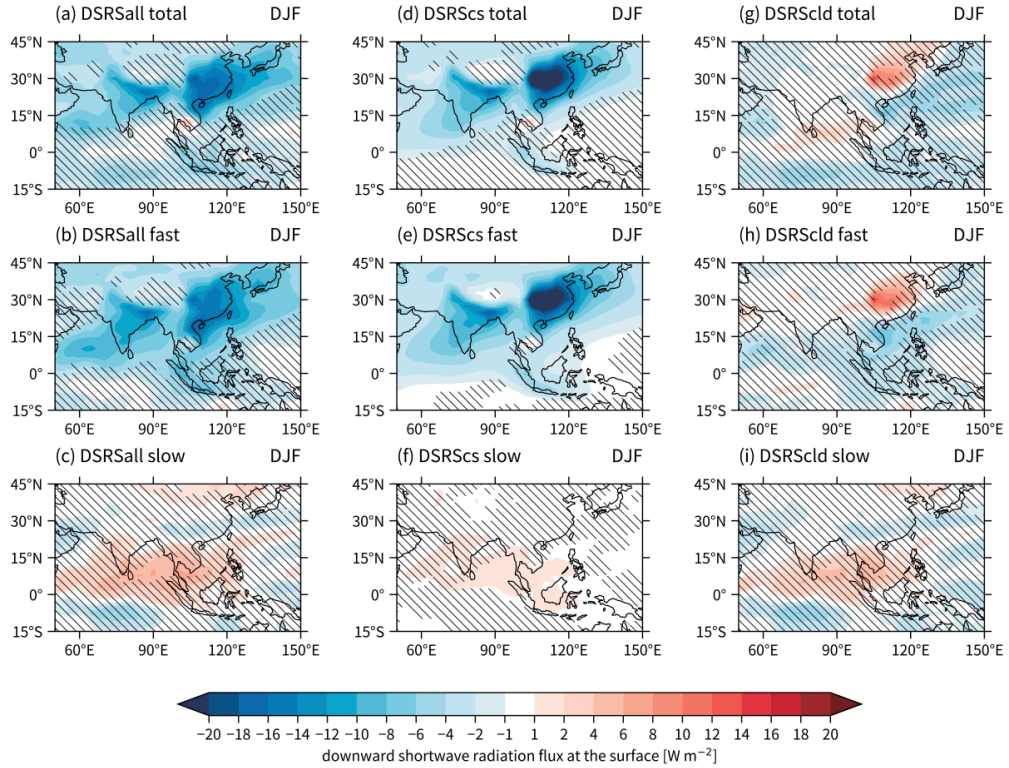

Fig. 4 **(a, d, g)** Total, **(b, e, h)** fast, and **(c, f, i)** slow responses of **(a–c)** all-sky DSRS, **(d–f)** clear-sky DSRS, and **(g–i)** difference of all-sky and clear-sky DSRS (cloud-related DSRS) in DJF. Hatching indicates regions with below 98% significance by sign test (not all modelensembles agreed on the sign).

4. Summary and Conclusion

We investigated the relative SAT warming over and around India induced by increasing AAs in DJF, although AAs generally cool SAT over and around the source regions. Using sets of CGCM and AGCM simulations of CMIP6, we separated the responses to increasing AAs into fast and slow responses. The relative SAT warming over and around India in DJF was significantly induced by the slow response. The slow response induced an interhemispherical gradient pattern in SAT, as shown in previous studies. A significant decrease in SAT_{fast} was observed over the AA source region.

Fast and slow responses of CL and vertical–meridional circulation over the Indian subcontinent were also compared. The slow response induced a decrease in CL and anomalous downward motions over India. There were anomalous upward motions over the South Indian Ocean, which enhanced climatological vertical–meridional circulation. However, the fast response induced none of these in DJF.

The $DSRS_{slow}$ increased over and around India through both cloud-related and non-cloud-related processes, whereas the $DSRS_{fast}$ decreased over and around India. From the perspective of the DSRS

response, $DSRS_{slow}$ was critical for the relative SAT warming in DJF. Therefore, the SST-mediated responses to AA decreased CL, and enhanced climatological vertical–meridional circulation, which in turn induced relative SAT warming over and around India. Moreover, the response of cloud-related processes was larger than that of non-cloud-related processes. Takahashi *et al.* (2018) emphasized the importance of the cloud precipitation processes, coupling with the dynamical process for the SAT response over South Asia to increasing AAs. Cloud-related processes can be important for SAT responses related to the relative SAT warming, which should be examined intensively.

References

Andrews, T., Forster, P. M., Boucher, O., Bellouin, N. and Jones, A. 2010. Precipitation, radiative forcing and global temperature change. *Geophysical Research Letters* **37**: L14701.

Bollasina, M. A., Ming, Y. and Ramaswamy, V. 2011. Anthropogenic aerosols and the weakening of the South Asian summer monsoon. *Science* **334**: 502–505.

Collins, W. J., Lamarque, J.-F., Schulz, M., Boucher, O., Eyring, V., Hegglin, M. I., Maycock, A., Myhre, G., Prather, M., Shindell, D. and Smith, S. J. 2017. AerChemMIP: Quantifying the effects of chemistry and aerosols in CMIP6. *Geoscientific Model Development* **10**: 585–607.

Eyring, V., Bony, S., Meehl, G. A., Senior, C. A., Stevens, B., Stouffer, R. J. and Taylor, K. E. 2016. Overview of the Coupled Model Intercomparison Project Phase 6 (CMIP6) experimental design and organization. *Geoscientific Model Development* **9**: 1937–1958.

Forster, P. M., Storelvmo, T., Armour, K., Collins, W., Dufresne, J.-L., Frame, D., Lunt, D. J., Mauritsen, T., Palmer, M. D., Watanabe, M., Wild, M. and Zhang, H. 2021. The Earth's energy budget, climate feedbacks and climate sensitivity. In *Climate Change 2021: The Physical Science Basis. Contribution of Working Group I to the Sixth Assessment Report of the Intergovernmental Panel on Climate Change*. eds. V. Masson-Delmotte, P. Zhai, A. Pirani, S. L. Connors, C. Péan, S. Berger, N. Caud, Y. Chen, L. Goldfarb, M. I. Gomis, M. Huang, K. Leitzell, E. Lonnoy, J. B. R. Matthews, T. K. Maycock, T. Waterfield, O. Yelekçi, R. Yu and B. Zhou, 923–1054. Cambridge University Press.

Ganguly, D., Rasch, P. J., Wang, H. and Yoon, J. 2012. Fast and slow responses of the South Asian monsoon system to anthropogenic aerosols. *Geophysical Research Letters* **39**: L18804.

Li, Z., Lau, W. K.-M., Ramanathan, V., Wu, G., Ding, Y., Manoj, M. G., Liu, J., Qian, Y., Li, J., Zhou, T., Fan, J., Rosenfeld, D., Ming, Y., Wang, Y., Huang, J., Wang, B., Xu, X., Lee, S.-S., Cribb, M., Zhang, F., Yang, X., Zhao, C., Takemura, T., Wang, K., Xia, X., Yin, Y., Zhang, H., Guo, J., Zhai, P. M., Sugimoto, N., Babu, S. S. and Brasseur, G. P. 2016. Aerosol and monsoon climate interactions over Asia. *Reviews of Geophysics* **54**: 866–929.

Takahashi, H. G., Watanabe, S., Nakata, M. and Takemura, T. 2018. Response of the atmospheric hydrological cycle over the tropical Asian monsoon regions to anthropogenic aerosols and its seasonality. *Progress in Earth and Planetary Science* **5**: 14.

Wang, H., Xie, S.-P., Kosaka, Y., Liu, Q. and Du, Y. 2019. Dynamics of Asian summer monsoon response to anthropogenic aerosol forcing. *Journal of Climate* **32**: 843–858.